



Use of SNPs with Controlled Size & Shape for Enhanced Surface Hydrophobicity & Hardness for Coil Coating Applications

Şevval Sulubaş

December, 2023

OUTLINE

- ❖ Introduction
- ❖ Materials & Method
- ❖ Characterization & Testing
- ❖ Findings
- ❖ Conclusion
- ❖ References

INTRODUCTION



Organic coatings are used mainly for protection and decoration

Coatings used in high speed lines to coat coils (metals shaped into foils and winded as a roll)



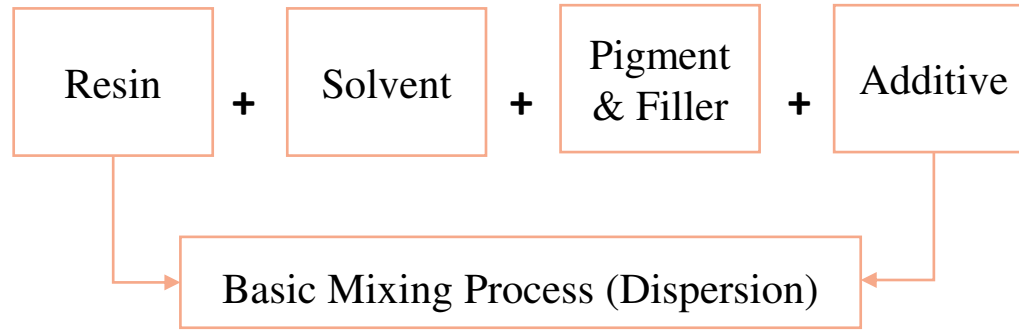
INTRODUCTION

- **Substrate:** HDG or Aluminium
- **Coating Line Speed:** 100 m/min (curing at 240 °C in 20-30 seconds)
- **Dry Film Thickness:** 5 micron primer + 20 micron topcoat (in general)

Application Areas of Coil Coatings



INTRODUCTION



Mechanical control

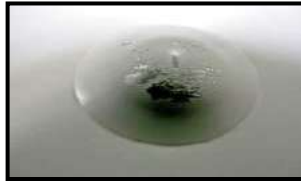


Fig 1. Impact Resistance Test



Fig 2. MEK Test

Color control

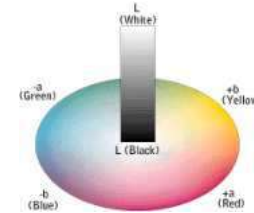


Fig 3. Color Control Test

INTRODUCTION

(Hydrophobic Coatings)

Hydrophobic surfaces has good water repellency and provide excellent properties such as:

- *Decreasing corrosion rate, easy to clean, self-cleaning, self healing properties etc.*

AIM OF THE STUDY

Synthesis of nano-inorganic particles to use in enhancing the hydrophobicity & hardness of coil coating surface.

HOW?

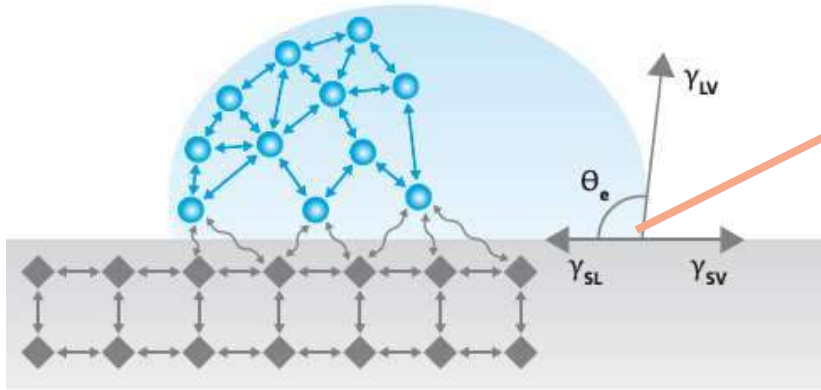
Creating roughness on the surface

INTRODUCTION

(Hydrophobic Coatings)

Wetting

- It is strong indicator for describing the interfacial relationships btw L & S & G.
- Liquid molecules interact more strongly with solid surface than the liquid.



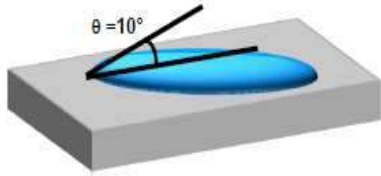
Contact Angle
Interfacial tensions form the equilibrium contact angle of wetting.

Young's Equation
Assumes surface is ideal (flat, smooth, chemically homogenous)

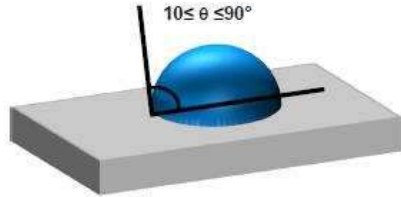
$$\gamma_{sv} = \gamma_{sl} + \gamma_{lv} \cos \theta_Y$$

Fig 4. Schematic diagram of interfacial tension in vapor/liquid/solid system (Wang et al., 2020)

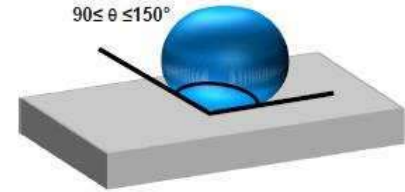
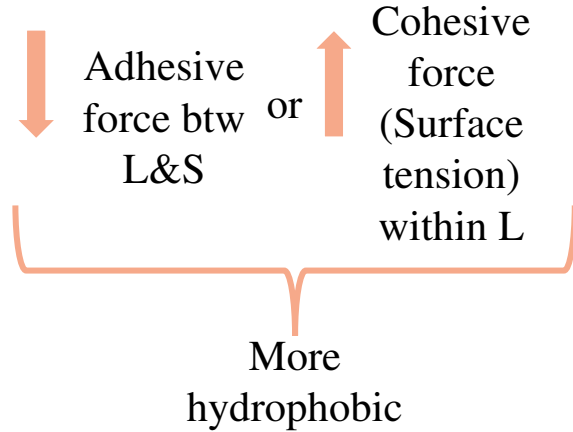
INTRODUCTION (Hydrophobic Coatings)



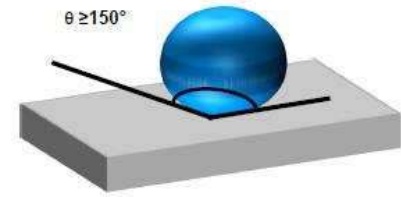
good wettability
(hydrophilic)



“normal” wettability



poor wettability
(hydrophobic)

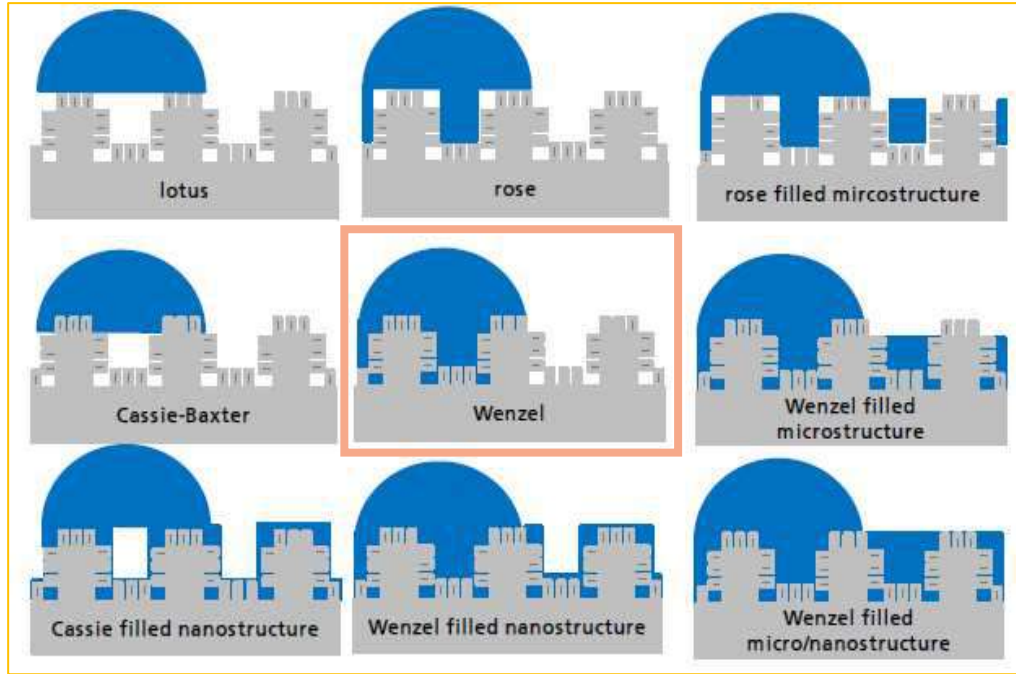


extremely poor wettability
(super-hydrophobic)



INTRODUCTION

(Hydrophobic Coatings)



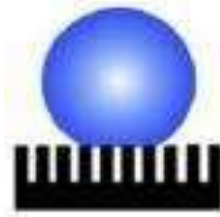
- There can be different states of water droplet on a rough surface.
- Surface roughness and morphology lead enhancement of hydrophobic behavior of the material.

Fig 5. Different wetting states (AkzoNobel Kemipol)

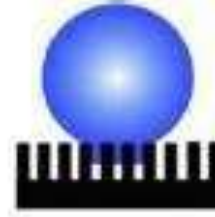
INTRODUCTION (Hydrophobic Coatings)



Wenzel's
state



Cassie's
state



Transitional state btw
Wenzel and Cassie



"Lotus"
state

$$\cos \theta_{rough} = r \cos \theta_{smooth}$$

$$\cos \theta_m = r \cos \theta_Y$$

r : roughness factor;

r=1 for smooth surface,

r>1 for rough surface

$$r = \frac{\text{Actual surface area}}{\text{Planar surface area}}$$

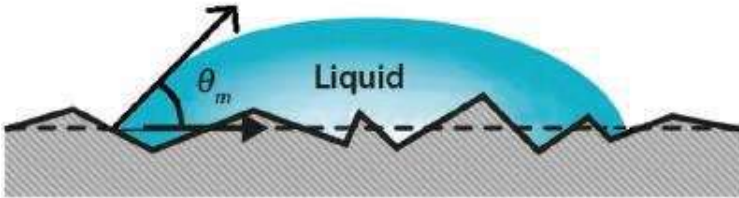


Fig 6. Apparent or measured contact angle on rough (Wenzel) surface (AkzoNobel Kemipol)

MATERIALS & METHOD

Synthesis & Characterization of SNP

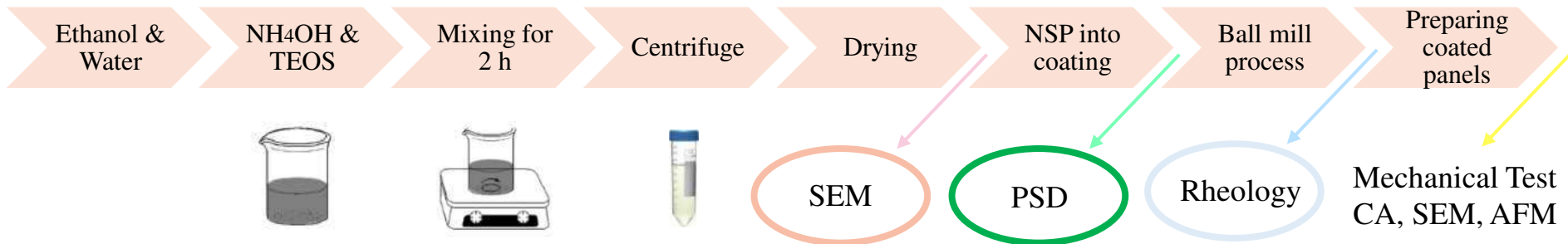
- Synthesis of silica by sol-gel / Stöber method and TEOS
- Characterization of SNP by SEM

Dispersion of SNP in coil coating

- Addition of NSP to PE coating mixture as a filler and dispersing.
- Characterization of coating mixture (Rheology, PSD)

Characterization of Coating

- Curing the coating for 40 sec at 240 °C and quenching
- Mechanical tests
- Surface characterization by CA & Surface energy measurements, SEM, AFM



Both monosize and multisize silica particles were added to coating mixture separately.

CHARACTERIZATION & TESTING

Monosize silica particles

- ❖ **Synthesis of Stöber Silica Particles**

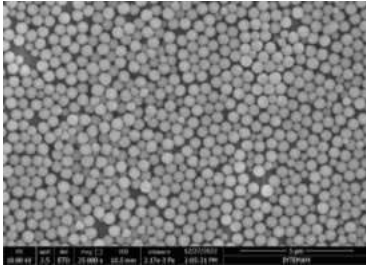
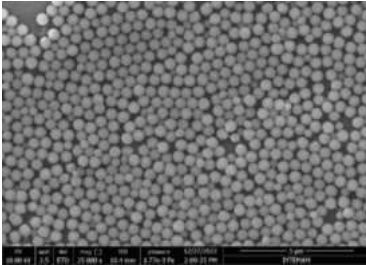
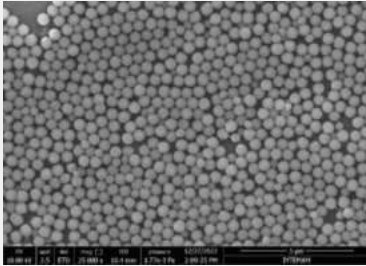
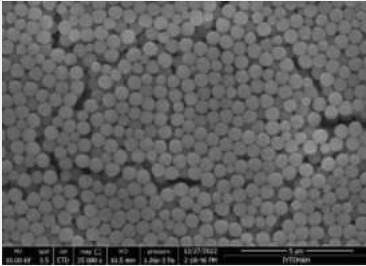
- ❖ *Effect of TEOS Concentration*

Bi-modal silica particles (Seed Addition / Seeded Growth)

CHARACTERIZATION & TESTING

(Synthesis of Stöber Silica Particles)

Table 1. SEM images of silica particles synthesized with different batches after 2 h and 24 h of synthesis

Sample	After 2 h	After 24 h
First Sample (100 ml)		
Second Sample (1 L)		

- ❖ Perfect spherical SNPs with 500-550 nm
- ❖ Repeatability & reproducibility for small & large scale samples
- ❖ Obtaining same particles after 2h and 24 h at the beginning of reaction

CHARACTERIZATION & TESTING

Monosize silica particles

❖ *Synthesis of Stöber Silica Particles*

❖ *Effect of TEOS Concentration*

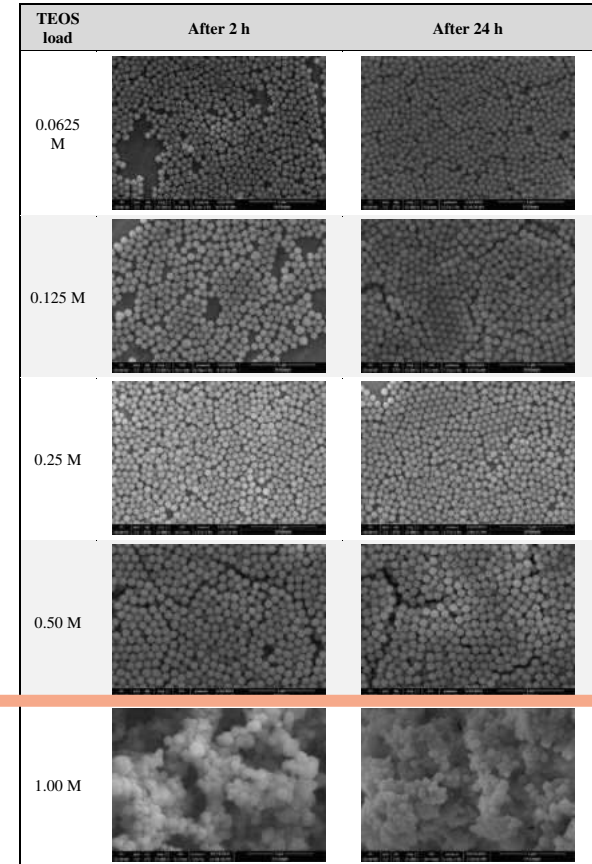
Bi-modal silica particles (Seed Addition / Seeded Growth)

CHARACTERIZATION & TESTING

(Effect of TEOS Concentration)

Table 2. Effect of TEOS concentrations

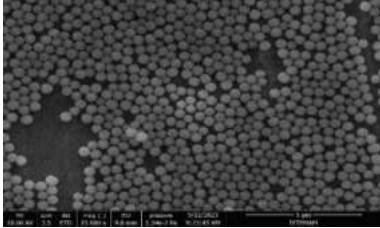
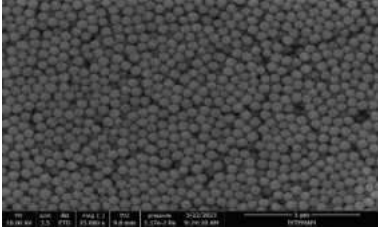
Parameters	Value
TEOS (mol/L)	0.0625M, 0.125M, 0.25 M , 0.50 M, 1 M
Ethanol (mol/L)	12.14 M
H ₂ O (mol/L)	11.67 M
NH ₃ (mol/L)	1.09 M



CHARACTERIZATION & TESTING

(Effect of TEOS Concentration)

Table 3. SEM images of effect of TEOS concentrations

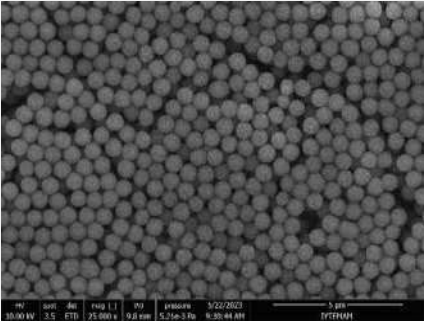
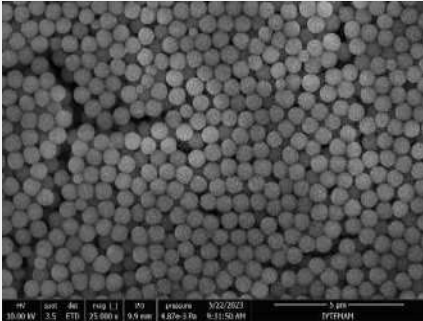
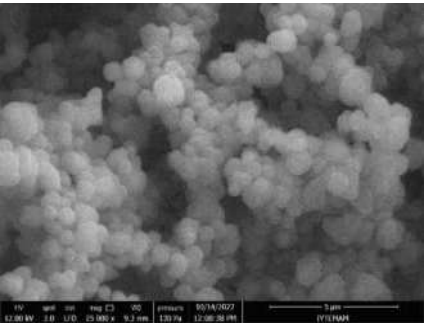
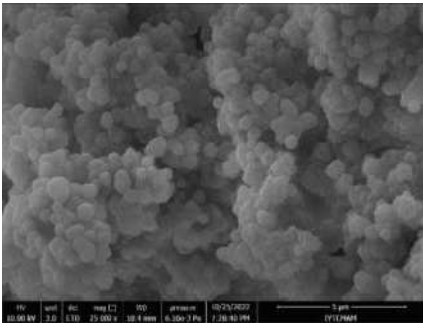
TEOS load	After 2 h	After 24 h
0.0625 M		

400-470 nm

CHARACTERIZATION & TESTING

(Effect of TEOS Concentration)

Table 4. SEM images of effect of TEOS concentrations

TEOS load	After 2 h	After 24 h
0.50 M		
1.00 M		

→ 590-620 nm
(*Silica D Method*)

→ Critical point

→ 400-700 nm
agglomeration

CHARACTERIZATION & TESTING

Monosize silica particles

❖ *Synthesis of Stöber Silica Particles*

❖ *Effect of TEOS Concentration*

Bi-modal silica particles (Seed Addition / Seeded Growth)

CHARACTERIZATION & TESTING

(Seed Addition / Seeded Growth)

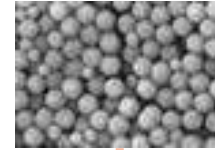
Synthesis of NSPs
(Stöber Formula)



Centrifuge
Process



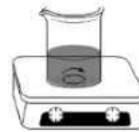
SNPs obtained
(seed particles)



Prepare new Stöber reaction
(TEOS free)



Seed Addition
(Directly)



TEOS Addition
(Pulse / Gradual)

Obtaining
Seeded Growth
Solution

CHARACTERIZATION & TESTING

(Seed Addition / Seeded Growth)

Table 5. Seed: Classic Stöber SNPs and their different growth solutions

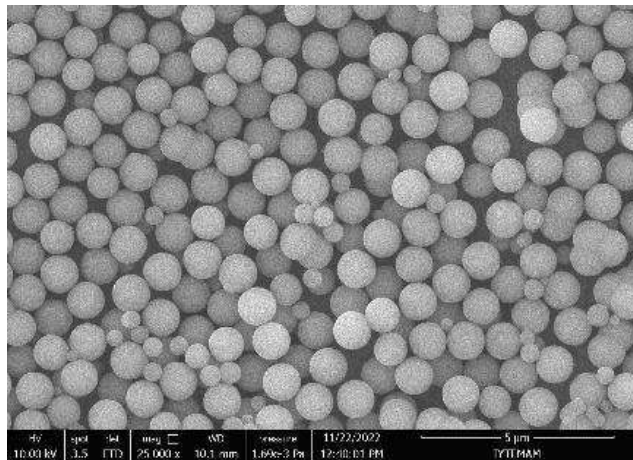
Method	After 2 h	Method	After 2 h
Seed: Stöber Method (Silica C) (500-550 nm)		2nd batch - Silica D Method (Obtained particles: 1.1 μm + 200 nm)	
1st batch – Classic Stöber Method with doubled TEOS and water concentrations (Obtained particles: 900 nm + 500-600 nm)		3rd batch - Silica D method with doubled TEOS and EtOH concentrations (Obtained particles: 650 – 750 nm)	

CHARACTERIZATION & TESTING

(Seed Addition / Seeded Growth)

Seed: Classic Stöber SNPs & growth solution with Silica D method

2nd batch - Silica D Method
(Obtained particles:
 $1.1\mu\text{m} + 200\text{ nm}$)



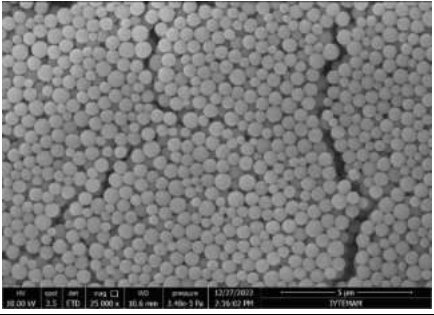
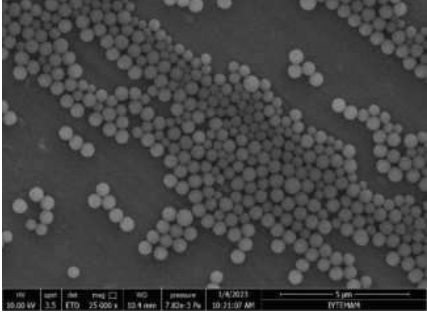
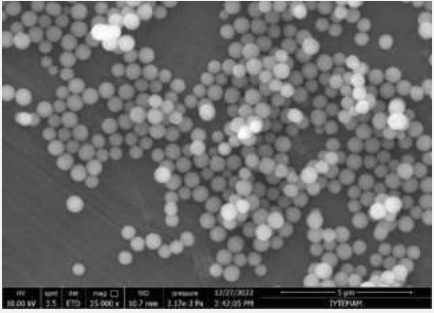
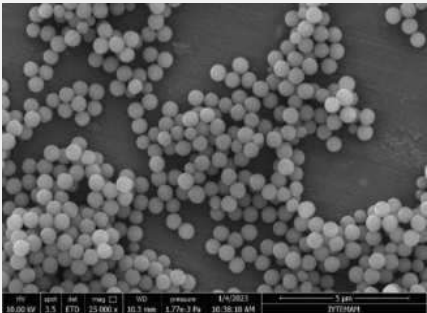
Particles with 200 nm smaller than the initial seed size. This indicates that new reactions were still ongoing, and a gradual addition of TEOS was necessary instead of a pulse addition.

CHARACTERIZATION & TESTING

(Seed Addition / Seeded Growth)

Preparing stock solution of SNPs

Table 6. SEM of stock solutions

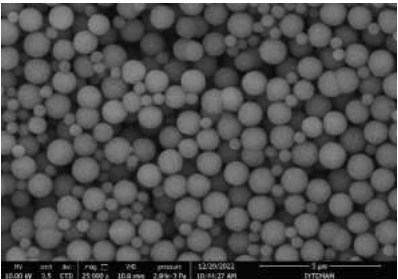
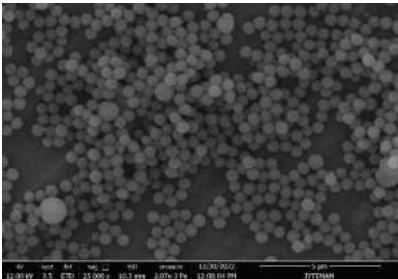
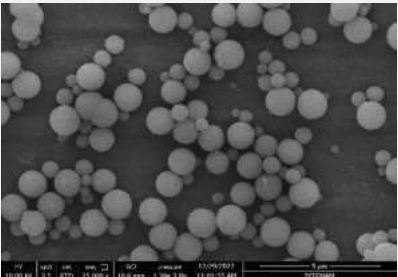
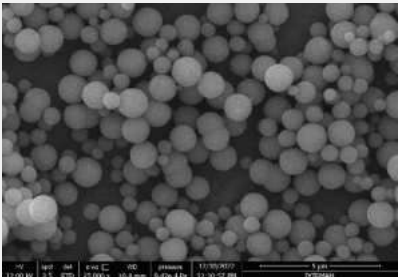
Seed Stock Stability	SEM Images	Seed Stock Stability	SEM Images
After 2 hours		After 2 weeks	
After 5 hours		After 2 months	

- ❖ Producing Stöber SNPs
- ❖ Preparing stock solution with a solid concentration of 15 g/L
- ❖ Short and long term stability

CHARACTERIZATION & TESTING

(Seed Addition / Seeded Growth)

Table 7. SEM of growth solutions (75 mg seed)

TEOS & EtOH	After 4 h	After 24 h
1 ml/min (Obtained particles: 1 μ + 200 nm)		
8 ml/min (Obtained particles: 1.2 μ + 200 nm)		

TEOS/EtOH ratio: 1/10

Addition rate: 1 & 8 ml/min

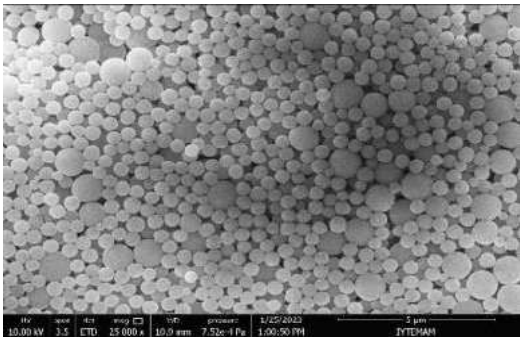
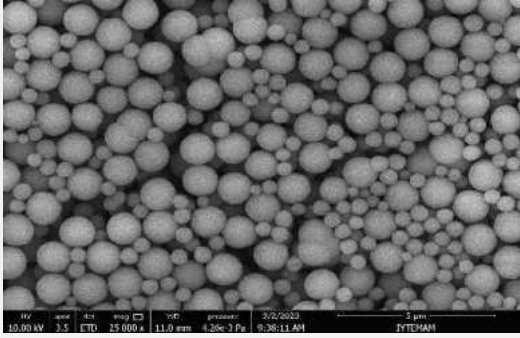
Seed amount: 75 mg Stöber SNPs

TEOS molecules started generating smaller nanoparticles around 500 nm instead of diffusing through the seed particles for growth. Therefore, overnight duration was required to complete the reaction and diffusion processes.

CHARACTERIZATION & TESTING

(Seed Addition / Seeded Growth)

Table 8. SEM of growth solutions (150 mg seed)

TEOS&EtOH (1/10) addition rate	After 24 h
1 ml/min (Obtained particles: 1 μ + 300-500 nm)	 <p>SEM image showing a dense field of spherical particles. The particles exhibit a bimodal size distribution with a primary population of approximately 1 μm and a secondary population of smaller particles (300-500 nm). The image includes technical data at the bottom: HV: 10.00 kV, spot: 3.5, ETO: 25,000 x, 10.0 mm, 7.52e-11 Pa, 1/25/2022, 1:00:50 PM, 5 μm, FYTESMAN.</p>
8 ml/min (Obtained particles: 1.2 μ + 550 nm)	 <p>SEM image showing a dense field of spherical particles. The particles exhibit a bimodal size distribution with a primary population of approximately 1.2 μm and a secondary population of smaller particles (550 nm). The image includes technical data at the bottom: HV: 10.00 kV, spot: 3.5, ETO: 25,000 x, 11.0 mm, 1.25e-11 Pa, 3/2/2023, 9:28:11 AM, 5 μm, FYTESMAN.</p>

TEOS/EtOH ratio: 1/10

Addition rate: 1 & 8 ml/min

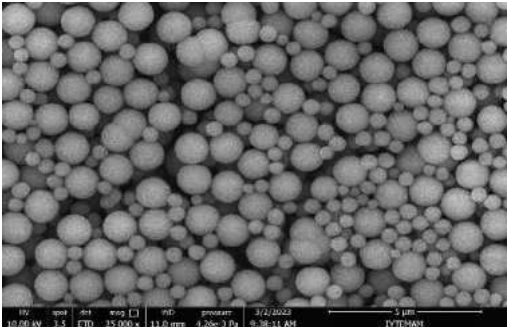
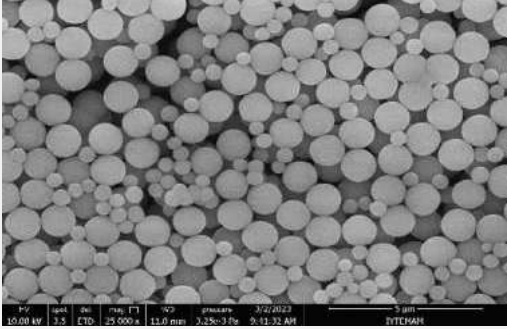
Seed amount: 150 mg Stöber SNPs

Rate of 8 ml/min: more equal size distribution

CHARACTERIZATION & TESTING

(Seed Addition / Seeded Growth)

Table 9. SEM of 100 ml & 1L growth solutions (150 mg seed)

TEOS&EtOH (1/10) addition rate	After 24 h
8 ml/min 100 ml solution (Obtained particles: 1.2 μ + 550 nm)	 <p>SEM image showing spherical particles. Technical data: HV: 10.00 kV, spot: 3.5, det: ETD, mag: 15,000x, WD: 11.0 mm, pressure: 4.20e-3 Pa, 3/2/2023, 9:28:11 AM, DITCHMAN. Scale bar: 5 μm.</p>
8 ml/min 1.5 L solution (Obtained particles: 1.2 μ + 550 nm)	 <p>SEM image showing spherical particles. Technical data: HV: 10.00 kV, spot: 3.5, det: ETD, mag: 25,000x, WD: 11.0 mm, pressure: 3.25e-3 Pa, 3/2/2023, 9:41:32 AM, DITCHMAN. Scale bar: 5 μm.</p>

TEOS/EtOH ratio: 1/10

Addition rate: 8 ml/min

Seed amount: 150 mg Stöber SNPs

Both 100 ml and 1.5 L solutions to control reproducibility

CHARACTERIZATION & TESTING (Coating Studies)

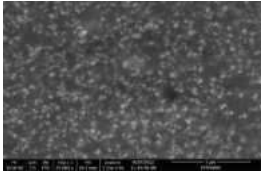
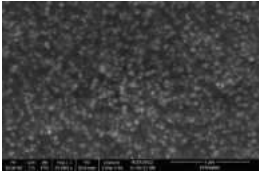
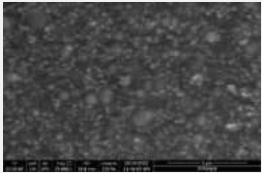
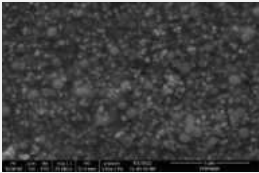
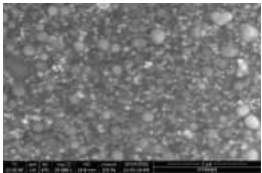
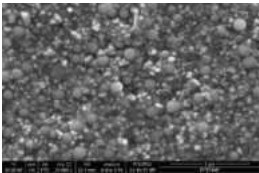
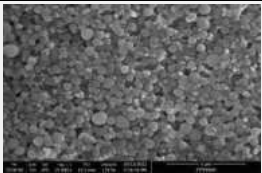
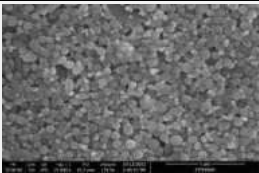
Monosilica Addition to Topcoat

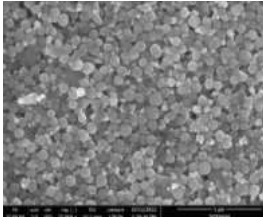
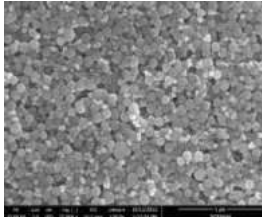
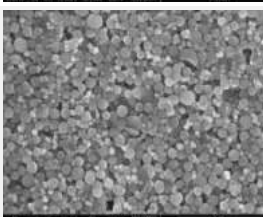
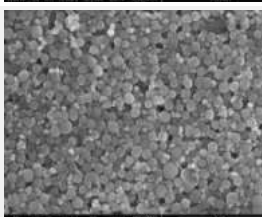
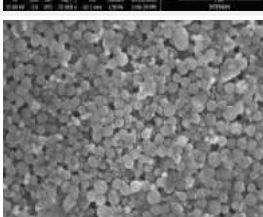

Bi-modal silica Addition to Topcoat

CHARACTERIZATION & TESTING

(Coating Studies – Monosilica Addition)

Table 10. SEM of monosilica added coating samples

Sample	SEM images for 20 μm film	SEM images for 10 μm film
5% Added SNPs		
15% Added SNPs		
20% Added SNPs		
25% Added SNPs		

Sample	SEM images for 20 μm film	SEM images for 10 μm film
30% Added SNPs		
40% Added SNPs		
45% Added SNPs		

similar
images with
25% added
SNPs

CHARACTERIZATION & TESTING

(Coating Studies – Monosilica Addition)

Table 11. CA for 20 & 10 μm films

Loading	Monosize - 20 mikron	Monosize - 10 mikron
45%	113.61	111.90
40%	113.54	110.80
35%	112.00	109.50
30%	110.50	105.42
25%	107.60	107.34
20%	92.00	92.71
15%	87.66	87.25
10%	86.32	84.2
5%	85.45	83.50
0%	82.20	82.20

Contact Angle Measurements

Table 12. Roughness Parameters & Actual Contact Angle

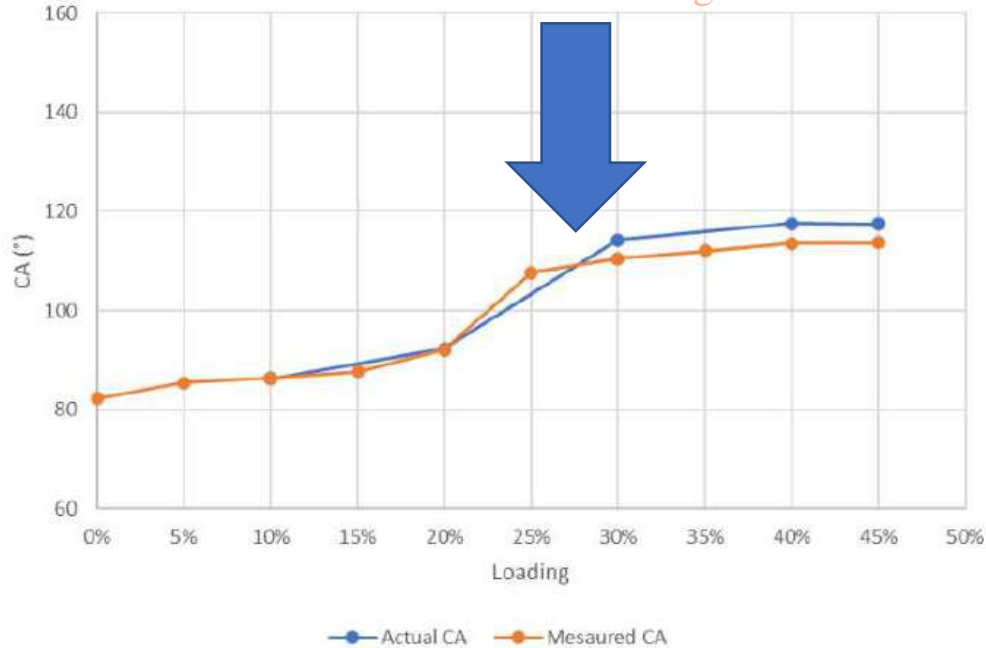
Sample	Projected Surface Area (μm ²)	Textured Surface Area (μm ²)	Roughness Parameter	Measured Contact Angle (°)	Actual Contact Angle (°)
45%	25.00	28.81	1.15	113.61	117.49
40%	25.00	28.98	1.16	113.54	117.58
30%	25.00	29.35	1.17	110.5	114.28
20%	25.00	28.25	1.13	92.00	92.26
10%	25.00	25.52	1.02	86.32	86.24

$$\cos \theta_m = r \cos \theta_y$$

$$r = \frac{\text{Actual surface area}}{\text{Planar surface area}}$$

CHARACTERIZATION & TESTING (Coating Studies – Monosilica Addition)

Contact Angle Measurements



Obtaining 90° between 15-20 %

Not dramatically increasing after loading of 25%

Maximum obtained CA: 113.61° at 45%

Fig 7. Contact Angle vs Silica Loading %

CHARACTERIZATION & TESTING

(Coating Studies – Monosilica Addition)

Mechanical Tests

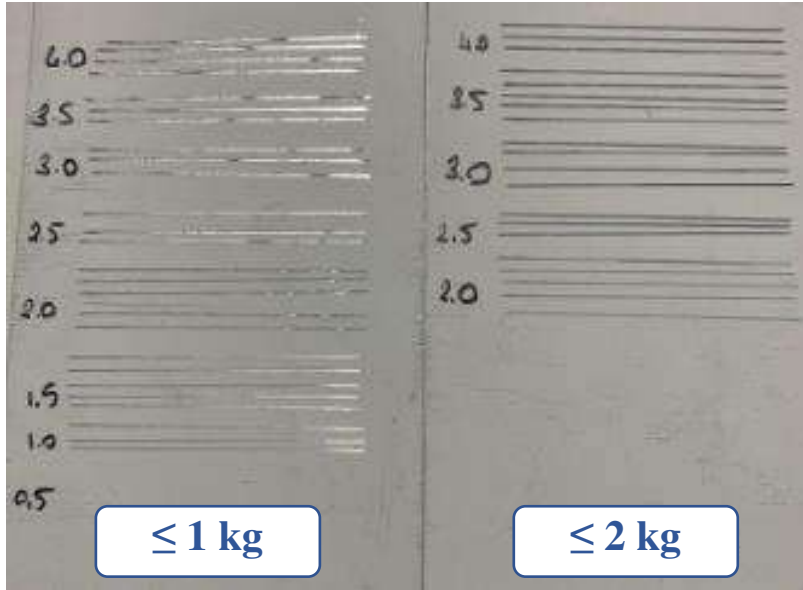


Fig 8. Scratch resistance results of 25 % and 30 % monosize silica added samples respectively

Table 13. Pencil hardness results of both 20 μm and 10 μm

Sample	Results of 20 micron	Results of 10 micron
0 - 35 %	2H	2H
40 - 45 %	3H	3H



CHARACTERIZATION & TESTING (Coating Studies)

Monosilica Addition to Topcoat

Bi-modal silica Addition to Topcoat

CHARACTERIZATION & TESTING

(Coating Studies – Bi-modal Silica Addition)

Table 14. AFM & SEM results of bi-modal SNPs added coating samples

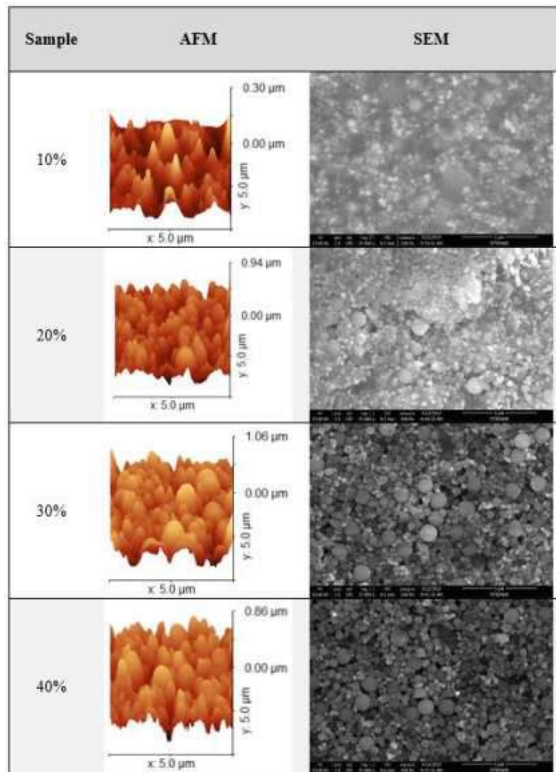


Table 15. CA for 20 & 10 μm films

Load	Bi-modal 20 μm	Bi-modal 10 μm
40%	116.70	111.50
35%	104.30	114.30
30%	108.40	110.50
25%	107.90	109.90
20%	106.10	106.40
15%	87.90	90.40
10%	88.30	88.50
5%	88.20	89.70
0%	82.20	82.20

Table 16. Roughness Parameters & Actual Contact Angle

Sample	Projected Surface Area (μm ²)	Textured Surface Area (μm ²)	Roughness Parameter	Measured Contact Angle (°)	Actual Contact Angle (°)
40%	25.00	44.13	1.77	116.70	142.48
30%	25.00	42.64	1.71	108.40	122.57
20%	25.00	38.85	1.55	106.10	115.53
10%	25.00	25.96	1.04	88.30	88.24

CHARACTERIZATION & TESTING

(Coating Studies – Bi-modal Silica Addition)

Contact Angle Measurements

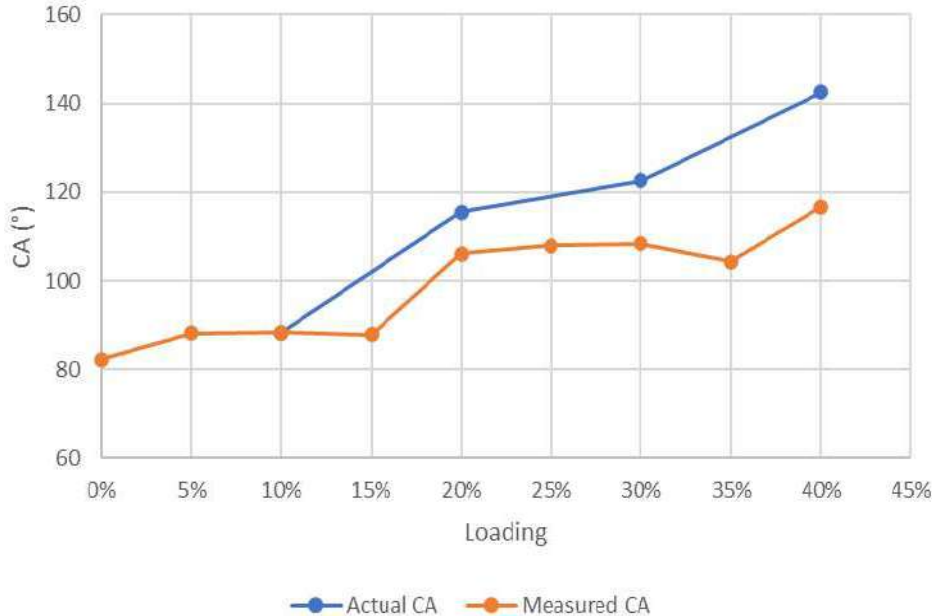


Fig 9. Contact Angle vs Silica Loading %

Obtaining 90° between 10-15 %

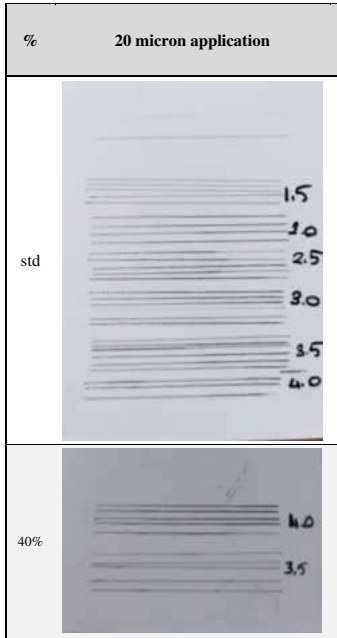
Maximum obtained CA: 116.7°
at 40%

Maximum CA: 142.48° by
considering roughness parameter

CHARACTERIZATION & TESTING

(Coating Studies – Bi-modal Silica Addition)

Mechanical Tests



$\leq 1 \text{ kg}$

$\leq 4 \text{ kg}$

Table 17. Pencil hardness results of both 20 μm and 10 μm

Sample	Results of 20 micron	Results of 10 micron
0 - 20 %	2H	2H
20 - 40 %	3H	3H

↑
Loading of
multisize
SNPs

↑
More hydrophobic
& harder coating
surface

Bi-modal silica particles have more effect on improving the scratch resistance of the surface than mono-size SNPs.

FINDINGS

Mono (550 nm) and bi-modal (550-1200 nm) nano silica particles were synthesized and employed as additives to increase the hardness and contact angle simultaneously in commercial coil coatings.

FINDINGS

The CA value of standard coat was 82° . It was increased to 113.61° with 45% monosized silica addition.

Monosized silica nanoparticles (35%) resulted in a surface hardness of 2H.

Increasing the loading to 45% improved the surface hardness to 3H.

40% addition of monosize silica was necessary to achieve a pencil hardness of 3H.

FINDINGS

Highest CA value achieved was 116.7° with addition of 40% bi-modal nano silica particles.

Incorporating the roughness parameter implies an effective CA value of 140° .

20% addition of bi-modal silica was sufficient to achieve a surface hardness of 3H.

CONCLUSION

Addition of silica nano particles simultaneously improves hardness and surface hydrophobicity in coil coating applications.

Bi-modal silica nano particles results in better contact angle and surface hardness performance compared to mono-modal particle size distribution.

ACKNOWLEDGEMENT

I would like to thank the following people, without whom I would not have been able to complete this research.

*Izmir Institute of Technology, especially to my supervisors **Prof. Dr. Mehmet Polat & Prof. Dr. Hürriyet Polat***

*Akzonobel Kemipol - Coil Coating R&D Team and Laboratory Team, especially to **İlkin Ece Altaş, Yağız Uysal, Hakan Ayyıldız, Ecem Tarancı, Cemre Kocahakimoğlu, Ender Kara, Gülçin Koşan***

*Izmir Institute of Technology, **TAM Members***

*Kansai Altan - **Physicochemistry Laboratory Team***

*And my biggest thanks to **my family** for all the support you have shown me through this research.*



REFERENCES

AkzoNobel Kemipol, Internal Documents

Alessi, A., Agnello, S., Buscarino, G., & Gelardi, F. M. (2013). Raman and IR investigation of silica nanoparticles structure. *Journal of Non-Crystalline Solids*, 362(1), 20–24. <https://doi.org/10.1016/j.jnoncrysol.2012.11.006>

Bai, Y., Zhang, H., Shao, Y., Zhang, H., & Zhu, J. (2021). Recent progresses of superhydrophobic coatings in different application fields: An overview. *Coatings*, 11(2), 1–30. <https://doi.org/10.3390/coatings11020116>

Bailey, J. K., & Mecartney, M. L. (1992). Formation of colloidal silica particles from alkoxides. *Colloids and Surfaces*, 63(1–2), 151–161. [https://doi.org/10.1016/0166-6622\(92\)80081-C](https://doi.org/10.1016/0166-6622(92)80081-C)

Bari, A. H., Jundale, R. B., & Kulkarni, A. A. (2020). Understanding the role of solvent properties on reaction kinetics for synthesis of silica nanoparticles. *Chemical Engineering Journal*, 398(March), 125427. <https://doi.org/10.1016/j.cej.2020.125427>

Branda, F., Silvestri, B., Luciani, G., & Costantini, A. (2007). The effect of mixing alkoxides on the Stöber particles size. *Colloids and Surfaces A: Physicochemical and Engineering Aspects*, 299(1–3), 252–255. <https://doi.org/10.1016/j.colsurfa.2006.11.048>

REFERENCES

- Busquets, J., Peláez, N., Gil, M., Secanella, L., Ramos, E., Lladó, L., & Fabregat, J. (2016). Is Pancreaticoduodenectomy a Safe Procedure in the Cirrhotic Patient? *Cirugía Española (English Edition)*, 94(7), 385–391. <https://doi.org/10.1016/j.cireng.2016.01.002>
- Bogush, G., Tracy, M., & Zukoski, C. (1988). Preparation of monodisperse silica particles: Control of size and mass fraction. *Journal of Non-Crystalline Solids*, 104(1), 95-106. [https://doi.org/10.1016/0022-3093\(88\)90187-1](https://doi.org/10.1016/0022-3093(88)90187-1)
- Bogush, G., & Zukoski, C. (1991). Uniform silica particle precipitation: An aggregative growth model. *Journal of Colloid and Interface Science*, 142(1), 19-34. [https://doi.org/10.1016/0021-9797\(91\)90030-c](https://doi.org/10.1016/0021-9797(91)90030-c)
- Chakraborty, D., Dingari, N. N., & Chakraborty, S. (2012). Combined effects of surface roughness and wetting characteristics on the moving contact line in microchannel flows. *Langmuir*, 28(48), 16701–16710. <https://doi.org/10.1021/la303603c>
- Chang, S. M., Lee, M., & Kim, W. (2005). Preparation of large monodispersed spherical silica particles using seed particle growth. *Journal of Colloid and Interface Science*, 286(2), 536-542. <https://doi.org/10.1016/j.jcis.2005.01.059>
- Chen, S. L., Dong, P., Yang, G. H., & Yang, J. J. (1996a). Characteristic aspects of formation of new particles during the growth of monosize silica seeds. *Journal of Colloid and Interface Science*, 180(1), 237–241. <https://doi.org/10.1006/jcis.1996.0295>

REFERENCES

Tunçgenç, M., (2004). Boya Teknolojisine Giriş

Saarimaa, V., Markkula, A., Juhanoja, J., & Skrifvars, B. J. (2015). Improvement of barrier properties of Cr-free pretreatments for coil-coated products. *Journal of Coatings Technology and Research*, 12(4), 721–730. <https://doi.org/10.1007/s11998-015-9663-6>

Stöber, W., Fink, A., & Bohn, E. (1968). Controlled growth of monodisperse silica spheres in the micron size range. *Journal of Colloid and Interface Science*, 26(1), 62-69. [https://doi.org/10.1016/0021-9797\(68\)90272-5](https://doi.org/10.1016/0021-9797(68)90272-5)

Völz, H. G. (2001). *Industrial color testing: Fundamentals and techniques*. Wiley-VCH Verlag GmbH.

Wang, J., Wu, Y., Cao, Y., Li, G., & Liao, Y. (2020). Influence of surface roughness on contact angle hysteresis and spreading work. *Colloid and Polymer Science*, 298(8), 1107–1112. <https://doi.org/10.1007/s00396-020-04680-x>

Yilgör, I., Lgor, S. Y., Lgor, E. Y., Yilgör, E., Soz, C. L., & Söz, Ç. K. (2016). Superhydrophobic polymer surfaces: Preparation, properties and applications.

Zeno W. Wicks, J., Jones, F. N., Pappas, S. P., & Wicks, D. A. (2007). *Organic coatings: Science and technology*. John Wiley & Sons.

Zhang, Y., Cao, M., Yao, Z., Wang, Z., Song, Z., Ullah, A., Hao, H., & Liu, H. (2015). Effects of silica coating on the microstructures and energy storage properties of BaTiO₃ ceramics. *Materials Research Bulletin*, 67, 70–76. <https://doi.org/10.1016/j.materresbull.2015.01.056>

